Journal of Advanced Mechanical Sciences (JAMS)
ISSN: 2583-3790 (Online)
"J. Adv. Mech. Sci., vol. 3, no. 1, pp. 35-50, (2024)"

Quasistatic Deformation of Shape Memory Rigid-Plastic Bodies under Variable External Loads and Temperatures

V. A. Grachev[1], Yu. S. Neustadt[2]*

[1,2]*Academy of Architecture and Building, Samara State Technical University, Samara, Russia*
**Corresponding Author Email and Phone Number: neustadt99@mail.ru*
Article received: 14/07/2024, Article Revised: 12/12/2024, Article Accepted: 30/12/2024
Doi: 10.5281/zenodo.14789889

Abstract

Plastic deformation plays a decisive role in inelastic deformation of solids. Therefore, it is appropriate to analyze mechanical behaviour within an ideal rigid plastic model with two loading surfaces. In the first section the problem of deformation of rigid plastic bodies is defined at the constant temperature in two equivalent forms: as a principle of virtual velocities and as a requirement of the minimum dissipative functional. In the second section the rigid plastic model of the solid is studied at the changing temperature with two loading surfaces. Two optimal principles are stated: for the force loading and for shape restoration. The existence of the generalized velocities is proved for 3D domains. The first and second laws of thermodynamics introduced in the design model enable the application of the variational principle at changing temperatures. In the third section shape memory materials are defined as solids with two loading surfaces. In conclusion problems for further studies are stated.

Keywords: *shape memory materials, rigid -plastic bodies, optimal principles, model with two loading surfaces, laws of thermodynamics, existence of generalized velocities.*

1. INTRODUCTION

At various temperatures θ, curves of relative extensions of central tie bars made of ideal elastoplastic shape memory materials depending on applied stresses σ are designated as ε = Ψ(σ) and are shown in Figure 1 as polygonal lines with arrows. Constants θ- and θ+ emphasize a range of temperatures, within which a specimen can restore its initial shape.

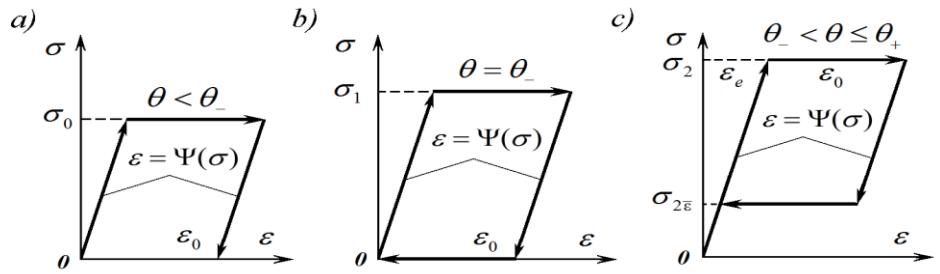

Figure 1. Curves $\varepsilon = \Psi(\sigma)$ (polygonal lines with arrows, σ — stress, ε — relative extension) of the bar made of elastoplastic shape memory material and elongated along one axis at

various temperatures θ. The stresses change on the graphs $\varepsilon = \Psi(\sigma)$ in the direction of the arrows: ***a)*** at low temperatures $\theta < \theta_-$, ε_0 is the residual deformation after the load removal; ***b)*** at shape restoration temperature θ_-: force loading under stress σ_1 and shape restoration when $\sigma = 0$; ***c)*** relationship between the stresses and relative deformations within the temperature range $\theta_- < \theta \leq \theta_+$: force loading under σ_2, shape restoration under $\sigma_{2\bar{\varepsilon}}$

If, shape memory solids are no different than ideal elastoplastic bodies: once unloaded, residual deformation is observed. When, 'reverse deformation' and slight elastic deformation, satisfying stress, are detected [1-3]. Experiments show that, therefore, can be taken in a first approximation and the rigid plastic element that underwent tension (Figure 2) can be reviewed.

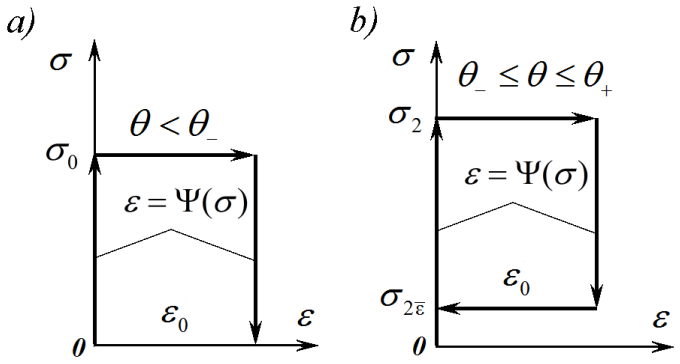

Figure 2: ***a)*** — tensile curve for the shape memory rigid plastic bar at low temperatures; ***b)*** — relationship between stress (σ) and deformation (ε) for the rigid plastic bar at "shape restoration temperatures $\theta_- \leq \theta \leq \theta_+$"

The behaviour of rigid plastic bodies at constant temperature θ < θ- has been reviewed in detail and is applicable to shape memory continuums (Figure 1a) under any loading. The purpose of this paper is to study deformation pattern of ideal shape memory materials in case of, when 'reverse deformation' occurs: heat supply eliminates residual deformation under low stresses. It is quite difficult to explain the behaviour of the solid (Figure 2a) based on the ultimate analysis of the elastoplastic model. In all known articles the solutions for the shape memory solids were found within type BD spaces (limited by the deformation) [4-6] using variational inequalities or variational principles like Reissner's. Basically, the existence and uniqueness of the solutions is proved under limited deformations. At the same time, big (ultimate) deformations are of main interest, when solids change their shape significantly. Besides, under ultimate deformations, the uniqueness of velocities is broken, which requires theoretical justification.

This paper offers direct analysis of the limit case based on some extension of the model of the elastoplastic solids. The process of deformation is studied phenomenologically without the theory of austenite-to-martensite transformations [7-10]. The objective is to explain the main behavioural characteristics of the shape memory solids observed during the experiments. First, the main points of deformation of rigid plastic bodies are defined at

constant temperature. Then the extended rigid plastic model with two loading surfaces is introduced. The existence of solutions for the accepted model is proved based on the main laws of thermodynamics. As a result, the deformation of the shape memory solids is explained within the theory of ideal plasticity.

2. PROPERTIES OF RIGID PLASTIC BODIES AT CONSTANT TEMPERATURE

The rigid plastic body D is defined as a 3D domain of the continuum in Cartesian coordinates $x_i\,(i=1,2,3)$ with the border $\partial D=\partial D_u+\partial D_p$. The part of the border ∂D_u is fixed, and external stress F_i are known on ∂D_p. In each point D velocity vector u_i and symmetrical stress tensor σ_{ij} are set. Using the velocity vector, the linear tensors of the deformation rates

$$\varepsilon_{ij}=\frac{1}{2}\left(\frac{\partial u_i}{\partial x_j}+\frac{\partial u_j}{\partial x_i}\right) \tag{1}$$

and relevant deviators $e_{ij}=\varepsilon_{ij}-\varepsilon,\ 3\varepsilon=\varepsilon_{ii}$ are calculated. Summation is done over the repeated subscript. The rigid plastic continuum is incompressible, therefore, $\varepsilon=0$ is postulated. Tensor σ_{ij} is associated with stress deviator s_{ij} by the equation

$$s_{ij}=\sigma_{ij}-\sigma,\ 3\sigma=\sigma_{ii} \tag{2}$$

Vector u_i is considered acceptable if it is a function of L_1 with the norm

$$\|u_i\|_{L_i}=\sum_{k}^{3}\int_D|u_k|dx+\sum_{k,m}^{1,2,3}\int_D\left|\frac{\partial u_k}{\partial x_m}\right|dx \tag{3}$$

and is equal to zero on the border ∂D_u. Here dx is a differential of volume.

Hereinafter, the ideal rigid plastic model by St. Venant-Levy-Mises [11-12] with the following properties is reviewed:

1. Tensor σ_{ij} exists only when deviator s_{ij} does not cross the boundaries of the loading surface within the nine-dimensional space

$$\Phi(s_{ij})=s_{ij}^2-2\tau^2=0 \tag{4}$$

where τ is a shear yield stress of the material.

2. If $s_{ij}^2<2\tau^2$, then $e_{ij}=0$.

3. If $s_{ij}^2-2\tau^2=0$, then $e_{ij}=\lambda s_{ij}$.

Thus,

$$\lambda = \frac{s_{ij} e_{ij}}{2\tau^2}, \quad s_{ij} = \frac{\sqrt{2}\,\tau\, e_{ij}}{\sqrt{e_{ij}^2}}. \tag{5}$$

Because of the above equation, deviator s_{ij} is determined by e_{ij} uniquely; the converse proposition is incorrect.

Besides, the following follows from (5)

$$s_{ij} = \frac{\partial \varphi}{\partial e_{ij}}, \quad \varphi(e_{ij}) = 2\tau (e_{ij}^2)^{1/2}. \tag{6}$$

Function φ is called a dissipative potential (function) corresponding to the loading function $\Phi(s_{ij})$.

Geometrical interpretation of the link between e_{ij} and s_{ij} is shown in Figure 3, where cross-section of surface $\Phi(s_{ij}) = 0$ with deviator plane $s_{33} = 0$ is presented in the main axes of deviator s_{ij}.

On the loading surface the direction of tensor e_{ij} coincides with the outer normal line and its second invariant is proportional to the power of the plastic deformation.

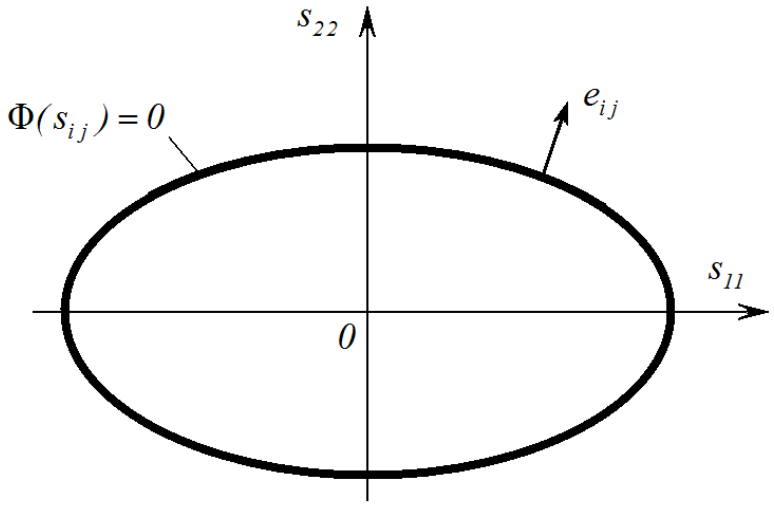

Figure 3. Cross-section of loading surface $\Phi(s_{ij}) = 0$ with deviator plane $s_{33} = 0$. Deviator of displacement velocities e_{ij} is normal to the loading surface.

If $\Phi(s_{ij}) < 0$, then $e_{ij} = 0$. Slow (quasistatic) movements of the rigid plastic continuum occur in accordance with the principle of virtual powers, i.e. the equality

$$\int_D s_{ij}\, e_{ij} dx = \int_D f_i\, u_i\, dx + \int_{\partial D_p} F_i\, u_i\, dS \tag{7}$$

holds for every geometrically acceptable u_i, that are connected to s_{ij} with equation (5).

Let us designate the set of permissible velocities u_i as P. In the equation (7) dS is a differential of the surface area ∂D_p, f_i is a load intensity per unit volume and F_i is an intensity of external forces on surface ∂D_p.

It is established [13] that the search for solutions to (7) equals to the problem of the functional minimum

$$J(e_{ij}) = \int_D \varphi(e_{ij}) dx - \int_D f_i\, u_i\, dx - \int_{\partial D_p} F_i\, u_i\, dS \tag{8}$$

on the set of permissible velocities $u_i \in P$.

The set of numbers m_s (static coefficients) is introduced based on the equality

$$\int_D s^0_{ij}\, e_{ij}\, dx = m_s \left(\int_D f_i\, u_i\, dx + \int_{\partial D_p} F_i\, u_i\, dS \right), \tag{9}$$

that is done under actual loads f_i, F_i for every $u_i \in P$.

Additionally, in each point of domain D there is statically acceptable safe deviator s^0_{ij} (inside the loading surface $\Phi(s_{ij}) = 0$).

The other set of numbers m_k (kinematic coefficients) is calculated from the equation

$$\int_D \varphi(e_{ij})\, dx = m_k \left(\int_D f_i\, u_i\, dx + \int_{\partial D_p} F_i\, u_i\, dS \right) \tag{10}$$

for acceptable $u_i \in P$ and set loads f_i, F_i.

It is proved [13 -14] that the following limits exist

$$\sup_{\Phi(s^0_{ij})<0} m_s = \inf_{u_i \in P} m_k = m_* \tag{11}$$

and the below statements are valid:

1. When $m < m_*$ the problem of the minimum of the function

$$\inf_{u_i \in P} \left[\int_D \varphi(e_{ij}) dx - m \left(\int_D f_i u_i dx + \int_{\partial D_p} F_i u_i dS \right) \right] = \inf_{u_i \in P} \left[\int_D \varphi(e_{ij}) dx - m \int_D s^0_{ij} e_{ij} dx \right] \tag{12}$$

has only a trivial solution for any geometrically acceptable $u_i \in P$ because the safe deviator of stresses exists in all points of the body *D*.

2. When $m > m_*$, system (7) has no solutions because deviator s_{ij} must not be outside of the loading surface.

3. When $m = m_*$, the problem has a non-trivial solution for a larger class of functions than in equation (3). The number m_* is called an ultimate load coefficient, and the following equation is true

$$m_* = \inf_{u_i \in P} \left[\frac{\int_D \varphi(e_{ij})\, dx}{\int_D f_i u_i\, dx + \int_{\partial D_p} F_i u_i\, dS} \right] \tag{13}$$

Thus, the rigid plastic body can change its shape only when $m = m_*$, while the set u_i should be chosen from wider space than L_1. The latter results from the fact that the space with the norm (3) is not reflexive: $m \to m_*$ does not follow by weakly convergent sequence u_{in}, $n \to \infty$, to element u_i^0 from L_1. In other terms, there is no such sequence $\left\| u_{in} - u_i^0 \right\|_{L_1} \to 0$, that for any functional L_1^* from the space conjugate to L_1, the equality $\lim_{n\to\infty} L_1^*(u_{in}) = L_1^*(u_i^0)$ would hold.

The general pattern of the space completion $u_i \in L_1$ is as follows. Let us designate the set of vectors with the norm (3) as K and review the space of linear functionals K^* conjugated to it. One-to-one correspondence $K^*(u_i)$ is established between u_i and some functional from K^* based on the equation

$$\left| K^*(u_i) \right| = \left\langle K^*, u_i \right\rangle \tag{14}$$

In (14) the norm of the functional K^* on set K is on the left and the value of the functional K^* on function u_i is on the right. Let us choose the total separable set B^0 within K^*. Totality means that if $\left\langle L, e_{ij} \right\rangle = 0$ for every $L \in B^0$, then $e_{ij} = 0$. In this case the second conjugated space $B^{0*} = M$ is the required extension. The convergence in norm (3) should be replaced with the weak* sequential convergence

$$\lim_{n\to\infty} \left\langle u_{in}, K^* \right\rangle = \left\langle u_i^0, K^* \right\rangle \tag{15}$$

Functional $J(e_{ij})$ increases on M

$$J(e_{ij}) \to \infty, \quad e_{ij} \in M \tag{16}$$

Besides, $J(e_{ij})$ is weakly* semi-continuous on M, i.e. for every sequence of $e_{ij}^n \in M$, weakly convergent to e_{ij}, the following equation holds

$$\underline{\lim}_{n\to\infty} J(e_{ij}^n) \geq J(e_{ij}) \tag{17}$$

Therefore, there is element $e_{ij} \in M$, where $J(e_{ij})$ reaches the lower bound m_*. The choice of B^0 is not unique. The subset of continuous functions can be defined as B^0, then B^{0*} is a set of measures where the existence of solutions to the rigid plastic problem was first proved [15]. Having defined B^0 as a set of bounded variation function, we obtain another class of solutions commonly occurring in practice, i.e. fields of vectors with finite jumps $[u_i]$ along internal surfaces S_τ. The main equations (7) is re-written as

$$\int_D s_{ij}\, e_{ij}\, dx + \int_{S_\tau} \tau [u_i]\, dS_\tau = \int_D f_i\, u_i\, dx + \int_{\partial D_p} F_i\, u_i\, dS = \dot{A}_{ext}. \tag{18}$$

The static and kinematic coefficients are calculated per the formulas:

$$\int_D s_{ij}^0\, e_{ij}\, dx + \int_{S_\tau} \tau^0 [u_i]\, dS_\tau = m_s \left(\int_D f_i u_i\, dx + \int_{\partial D_p} F_i\, u_i\, dS \right), \tag{19}$$

$$\int_D \varphi(e_{ij})\, dx + \int_{S_\tau} \tau [u_i]\, dS_\tau = m_k \left(\int_D f_i\, u_i\, dx + \int_{\partial D_p} F_i\, u_i\, dS \right). \tag{20}$$

The ultimate load exists, and equations (11)–(13) are not changed. Hereinafter, they are going to be used as such. It should be noted that equality (18) means the law of conservation of energy (first law of thermodynamics) on the actual velocity field u_i and at constant temperature, if

$$\int_D s_{ij}\, e_{ij}\, dx + \int_{S_\tau} \tau [u_i]\, dS_\tau = \dot{L}_{int}$$

is the rate of internal energy variation. In case of no heat supply $\dot{Q}$, the first law of thermodynamics

$$\dot{E} = \dot{Q} + \dot{A} \tag{21}$$

turns into equality $\dot{L}$ [illegible]

The second law of thermodynamics in the form of the Clausius statement at constant temperature

$\dot{L}$ [illegible] (22)

where H is an entropy (calorie per [16]) that also holds because of non-negativity of $\dot{E}(u_i)$. Thus, the variational principle (18) describes the behavior of the rigid plastic continuum at constant temperature without the laws of thermodynamics.

The previous reviews demonstrate that the problem of the minimum functional

$$\inf_{u_i \in P}\left[\int_D \varphi(e_{ij})\,dx + \int_{S\tau} \tau[u_i]\,dS_\tau - m\left(\int_D f_i u_i\,dx + \int_{\partial D_p} F_i u_i\,dS\right)\right] \tag{23}$$

always has solutions like $u_i = Cu_i^0$, where C is invariable because φ is a homogeneous function of first degree $\varphi(Cu_i) = C\varphi(u_i)$. Normalization $\|u_i\| = 1$ is usually chosen for the invariable C. The analog of the second law of thermodynamics seems more physically based: when the internal energy dissipates in atmosphere (at constant temperature), there is such an invariable C_0 that the following inequality holds

$$\int_D \varphi(e_{ij})\,dx + \int_{S_\tau} \tau[u_i]\,dS_\tau \le C_0 \int_D dx. \tag{24}$$

Once velocities u_i are estimated, the displacements of body points w_i are calculated by integration of the equations

$$\frac{dw_i}{dt} = u_i(x). \tag{25}$$

These equations can be solved on the time interval $0 \le t \le T$ within the same generalized extensions $B^{0*} = M$ of the initial space if functions u_i are measurable. In practice a finite number of intervals is normally used, with the constant value of u_i on each of them. to make integration (25) possible. Thereby, the problem of deformation of the shape memory rigid plastic continuum is solved when $\theta < \theta$.

3. RIGID PLASTIC BODIES WITH TWO LOADING SURFACES

Let us consider a continuum that can deform at constant temperature, only when the stresses at any point are located in the nine-dimensional space of deviators within the volume *R* limited by similar loading surfaces $\Phi(s_{ij}) = 0$ and $\Phi_0(s_{ij}) = 0$ (Figure 4).

The equations for the loading surfaces are as follows:

$$\Phi(s_{ij}) = s_{ij}^2 - 2\tau^2 = 0,\ \Phi_0(s_{ij}) = s_{ij}^2 - 2\tau_*^2 = 0,\ \tau_* = \beta\tau,\ 0 < \beta < 1. \tag{26}$$

If Π is an internal point on domain *R*, then $e_{ij} = 0$. If Π is located on the external border, then $e_{ij} = s_{ij}\sqrt{e_{ij}^2}/(\tau\sqrt{2})$, whereas $e_{ij}^0 = s_{ij}\sqrt{e_{ij}^2}/\tau_*\sqrt{2}$ on the internal border. Deviators e_{ij}, e_{ij}^0 are directed to the loading surfaces along the outward normal.

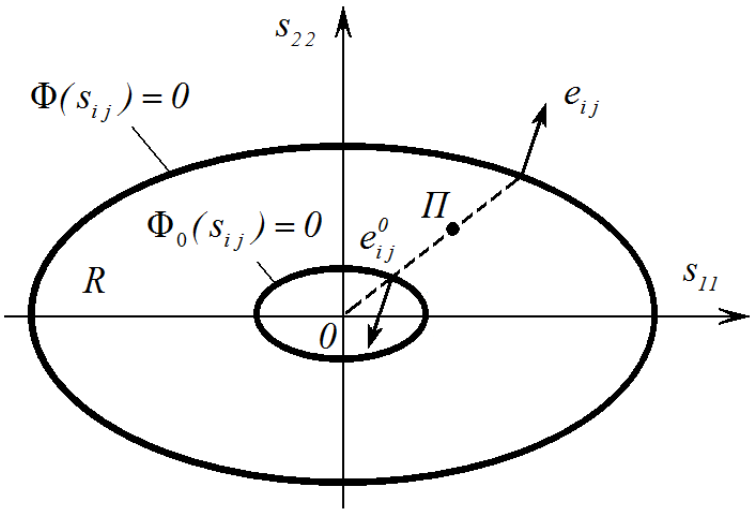

Figure 4. Cross-section of two loading surfaces with the deviation plane $\Phi(s_{ij})=0$ и $\Phi_0(s_{ij})=0$. Tensors e_{ij}, e^0_{ij} are normal to the loading surfaces, R is a domain of possible stress deviators, Π is an arbitrary point on domain R.

Formulas (26) and equations for e_{ij}, e^0_{ij} meet the requirement to orthogonality of thermodynamic forces and fluxes [17].

Let us associate the following dissipative functions with each loading surfaces:

$$\varphi(e_{ij})=2\tau\sqrt{e^2_{ij}}\ \ \varphi_0(e_{ij})=2\tau_*\sqrt{e^2_{ij}}. \qquad (27)$$

Figure 4 has a distinctive feature. If point Π moves in a straight line that passes through the origin of coordinates (proportional loading), the directions of tensors e_{ij}, e^0_{ij} differ by 180°. It could be interpreted as a shape memory on surface $\Phi_0(s_{ij})=0$ after deformation of the body with the forces according to configuration $\Phi(s_{ij})=0$.

Let the rigid plastic body be loaded with the forces (by analogy with the equation (7)). The loads are acceptable if deviator $\overline{s}_{ij}\in R$ exists and for every geometrically feasible u_i the following equality holds

$$\int_D \overline{s}_{ij}\, e_{ij}(u_i)\,dx=\int_D f_i u_i\,dx+\int_{\partial D_p} F_i u_i\,dS. \qquad (28)$$

Let us review the proportional loading by deviator $m\overline{s}_{ij}$. Two ultimate parameters $m=\{m^+_*, m^-_*\}$ will be calculated. When $m=m^+_*$, there is a non-zero allowable vector u^+_i for the following equation to be valid

$$\int_D s_{ij}\, e_{ij}(u_i^+)\,dx + \int_{S_\tau} \tau[u_i^+]\,dS_\tau = m_*^+ \left(\int_D f_i u_i^+\,dx + \int_{\partial D_p} F_i u_i^+\,dS \right) = m_*^+ \int_D \overline{s}_{ij}\, e_{ij}(u_i^+)\,dx \qquad (29)$$

and the conditions: $s_{ij} = \tau\sqrt{2}\, e_{ij} / \sqrt{e_{ij}^2}$, when $e_{ij} \neq 0$; $s_{ij} \in R$, when $e_{ij} = 0$.

In case of $m = m_*^-$, there is a non-zero vector u_i^-, when the equation

$$\int_D s_{ij}\, e_{ij}(u_i^-)\,dx + \int_{S_\tau} \tau[u_i^-]\,dS_\tau = m_*^- \left(\int_D f_i u_i^-\,dx + \int_{\partial D_p} F_i u_i^-\,dS \right) = m_*^- \int_D \overline{s}_{ij} e_{ij}(u_i^-)\,dx \qquad (30)$$

holds with the conditions: $s_{ij} = \tau_* \sqrt{2}\, e_{ij} / \sqrt{e_{ij}^2}$, when $e_{ij} \neq 0$; $s_{ij} \in R$, when $e_{ij} = 0$.

The values of m_*^+, m_*^- can be calculated through relevant static and kinematic coefficients. The static coefficient for m_*^+ is defined as:

$$\int_D s_{ij}^0\, e_{ij}\,dx + \int_{S_\tau} \tau^0[u_i]\,dS_\tau = m_s^+ \int_D \overline{s}_{ij}\, e_{ij}(u_i)\,dx, \text{ при } u_i \in P, \{ s_{ij}^0, \tau^0 \in \Phi(s_{ij}^0) < 0 \}. \qquad (31)$$

For m_*^- the similar equation is written as:

$$\int_D s_{ij}^0\, e_{ij}\,dx + \int_{S_\tau} \tau^0[u_i]\,dS_\tau = m_s^- \int_D \overline{s}_{ij}\, e_{ij}(u_i)\,dx, \text{ при } u_i \in P, \{ s_{ij}^0, \tau^0 \in \Phi_0(s_{ij}^0) > 0 \}.$$

Formulas for the kinematic coefficients are as follows:

$$\begin{aligned} &\int_D \varphi(e_{ij})\,dx + \int_{S_\tau} \tau[u_i]\,dS_\tau = m_k^+ \int_D \overline{s}_{ij}\, e_{ij}(u_i)\,dx,\ u_i \in P; \\ &\int_D \varphi_0(e_{ij})\,dx + \int_{S_\tau} \tau_*[u_i]\,dS_\tau = m_k^- \int_D \overline{s}_{ij}\, e_{ij}(u_i)\,dx,\ u_i \in P. \end{aligned} \qquad (32)$$

By analogy with (13) the limit relations hold

$$\sup_{\Phi(s_{ij}^0)<0} m_s^+ = \inf_{u_i \in P} m_k^+ = m_*^+, \quad \inf_{\Phi_0(s_{ij}^0)>0} m_s^- = \sup_{u_i \in P} m_k^- = m_*^- \qquad (33)$$

and non-trivial vectors u_i^+, u_i^-, obtained from the variational principles, are ensured to exist in B^{0*} extended classes

$$\inf_{u_i \in P} J^+(e_{ij}) = \inf_{u_i \in P} \left[\int_D \varphi(e_{ij})\,dx + \int_{S\tau} \tau[u_i]\,dS_\tau - m_*^+ \int_D \overline{s}_{ij}\, e_{ij}(u_i)\,dx \right] \qquad (34)$$

$$\sup_{u_i \in P} J^-(e_{ij}) = \sup_{u_i \in P} \left[\int_D \varphi_0(e_{ij})\,dx + \int_{S\tau} \tau_*[u_i]\,dS_\tau - m_*^- \int_D \overline{s}_{ij}\, e_{ij}(u_i)\,dx \right] \qquad (35)$$

Extremum principles (34), (35) equal to the initial setting of the problem regarding the existence of the solutions for the rigid plastic continuums with two loading surfaces (if the

problem is set in the form of the virtual power principle where possible stresses are limited by $s_{ij} \in R$). In other words, it is proved that, within the rigid plastic continuum with two loading surfaces, forces f_i, F_i cause non-trivial displacements only when the conditions (34), (35) and the equalities are satisfied.

$$m_*^+ = m_*^- = 1 \qquad (36)$$

Hereinafter we shall consider that the time of deformation $0 \le t \le T$ is split into the finite number of intervals, whereas one of the conditions $m_*^+ = 1$ or $m_*^- = 1$ is satisfied in each of them. The case of $m_*^+ = 1$ is seen similar to the plotting in section 2, when it is reasonable to use (24) as an additional requirement to normalization of the displacements and to consider the laws of thermodynamics (21), (22) to be satisfied automatically. When $m_*^- = 1$ (reverse deformation), the situation becomes more complicated because the laws of thermodynamics are not automatically satisfied on surface $\Phi_0(s_{ij}) = 0$ at moderate temperatures.

Validly, when heat is not supplied, there should be $\dot{E} = \dot{A}$ but $d\dot{A} = \tau_* \sqrt{e_{ij}^2}$, and the experiments demonstrate a value of $d\dot{A} = \gamma \tau \sqrt{e_{ij}^2}$, $\beta < \gamma \le 1$ for internal energy power.

In other words, in order to perform the reverse deformation, the work comparable to the force deformation has to be done. Using the analogy between the plastic flow and melting [18-19] it can be stated that the work to convert the rigid continuum into the plastic one (the flow under stress τ) is comparable to the work done during the reverse "flow-melting". Deformation of the continuum with two loading surfaces is very similar to the steel behavior at high temperatures, close to the melting point.

In Figure 5 the solid wavy line (number ***1***) describes the experimental curve for the shear yield stress of soft steel as a function of temperature, whereas number ***2*** is a dotted polygonal line used in technical melting calculations [20]. If the curve ***2*** is replaced with the similar solid thick main line ***3*** and the energy of reverse transformation for shape memory alloys is assumed to take intermediate value $2\gamma\tau\sqrt{e_{ij}^2}$, $\beta < \gamma < 1$, when the process runs under stresses τ_*, then the temperature, corresponding to $\sqrt{2}\tau_*$, can be called "shape restoration temperature. The latter hypothesis is equivalent to the existence of the "latent melting heat". It is natural to call number γ a "parameter of the reverse transformation latent heat". It should also be noted that interpretation of the shape memory materials as a solid continuum with two loading surfaces is close to hysteresis modeling by Preisach [21-23] in magnetic alloys.

Essentially, shape memory materials are upgraded alloys where the point of "reverse melting" is moved to the area of moderate temperatures. For such materials the first law of thermodynamics

$$\dot{L} \quad \dot{L} \quad \sqrt{e_{ij}^2}, \quad \sqrt{\quad_{ij}^2}. \tag{37}$$

explains the necessity of additional heat supply $\dot{Q} = \dot{E} - \dot{A} > 0$ for the "reverse flow" — shape restoration. In order to validate feasibility of work performance at the expense of the heat supply, the second law of thermodynamics, written in the Clausius form, should also be taken into account

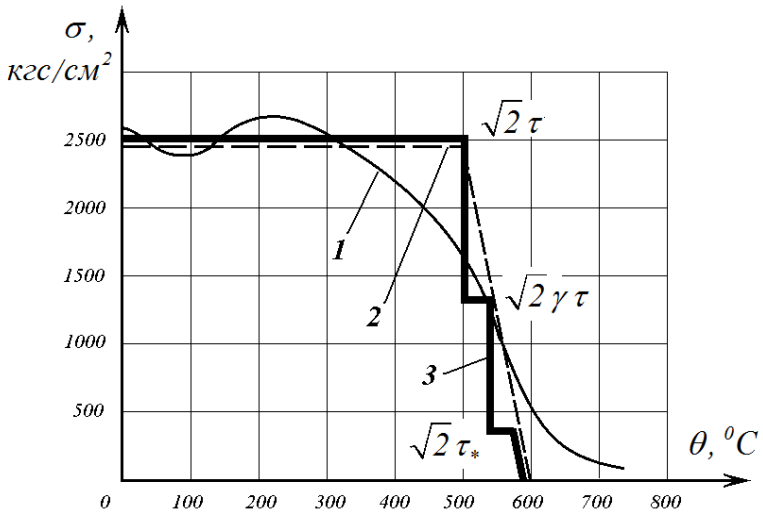

Figure 5. Shear yield stress of soft steel τ as a function of temperature θ when testing centrally compressed specimens (curves ***1, 2***) under stress σ and possibility to interpret the area between 500 and 600 ^{0}C with two loading surfaces: ***1*** is an experimental curve (solid wavy line); ***2*** is a simplified curve used in technical estimates (dotted line); 3 is a polygonal line corresponding to two loading surfaces τ and τ_* (solid thick main line); number γ is a "parameter of the reverse transformation latent heat"

$$\theta \dot{I} \quad \dot{\quad}. \tag{38}$$

Because there is no free energy $F = E - \theta H,$ then $\dot{L}$ and from (38) it follows that $\dot{\iota}$ The value H is estimated up to the constant accuracy, therefore, θ can be chosen so that $\dot{\quad}$ i.e. heat input performs the reverse operation.

4. PHENOMENOLOGICAL ANALYSIS OF SHAPE MEMORY RIGID PLASTIC CONTINUUMS

Let us consider that the material of body D has a shape memory if the following conditions are satisfied: M1. 3D manifold D is a rigid plastic continuum with two loading surfaces. Equations (26)–(34), connecting stresses and deformation rates, are satisfied. The external loads can be counterbalanced with deviator s_{ij}^-, and the equation $\Phi_0^\delta(s_{ij}^-) = s_{ij}^- s_{ij}^- - 2(\tau_* + \delta)^2 = 0, \quad \delta > 0, \ \tau_* + \delta < \tau$ holds.

M2. Function θ (absolute temperature), as well as constants τ and τ_*, which are experimental functions of θ, are defined within domain D.

M3. In case of $m_*^- = 1$ (shape restoration), the variational principle (35) is valid. Additionally, variables θ and u_i can be linked at any point of time $0 \le t \le T$ with the first law of thermodynamics and Fourier's thermal conduction law

$$\int_D [2\gamma\tau\sqrt{e_{ij}^2(u_i)} + c_1\rho\dot{\theta} - c_2\nabla^2\theta - \dot{q}\theta_{ij}(u_i)]dx = 0. \qquad (39)$$

where c_1 is heat capacity ratio, ρ is material density, c_2 is heat conductivity ratio, ∇^2 is Laplacian operator, q is density of applied heat per unit time.

If $m_*^+ = 1$ (force loading), the variational principle (34) holds under the condition (24), whereas the first law of thermodynamics turns into the heat conductivity equation: the applied heat changes the temperature of the solid per formula (40) without additional deformations

$$c_1\rho\dot{\theta} - c_2\nabla^2\theta = \dot{q} \qquad (40)$$

M4. The material "remembers" deviation from the initial position at any point of time and distributes the applied heat based on formula (39), only when the state of deformation differs from the original one. The "shape restoration" occurs: the direction of deviator e_{ij} from (39) is opposite to the remembered one.

The results from the previous section allow us to state that the solutions for the solids with M1–M4 properties exit. Validly, if the external forces are balanced with the stress deviator located within the domain R (Figure 4), the geometry of the domain does not change $e_{ij} = 0$, and the temperate is calculated from the equation (40). If deformation occurs according to M3, then (as stipulated before) velocities u_i can be estimated within extended space $B^{0*} = M$ per variational principles (34), (35) at any point of time. Taking density $\dot{q}$ from the same space and considering s_{ij}^- a continuous coordinate function means that the temperature can be selected from manifold $\theta \in M$. This conclusion follows from the possibility to explicitly solve equations (39)–(40) [24] relative to time using spectrum factorization of Laplacian operator Z

$$Z = \frac{c_2}{c_1\rho}\left(\frac{\partial^2\theta}{\partial x_1^2} + \frac{\partial^2\theta}{\partial x_2^2} + \frac{\partial^2\theta}{\partial x_3^2}\right), \qquad (41)$$

$$\theta(t,x) = exp((tZ)\Theta(x) + \int_0^t exp((t-s)Z)\times[\dot{q} - \tau\sqrt{e_{ij}^2(u_i(s))} - s_{ij}^- e_{ij}(u_i)]ds,$$

$$\exp((t-x)Z) = \sum_{k=0}^{\infty}((t-x)Z)^k/k!\ , \quad Z^k = \int_0^{\infty} v^k dE_v.$$

Letter Θ designates the initial temperature of the solid. The joint use of (35) and (39) can often be simplified because the shape is normally restored at constant temperature $\dot{\theta} = \nabla^2 \theta = 0$. Thus, the equation

$$2\gamma\tau\sqrt{e_{ij}^2(u_i)} + \dot{c} \quad {}_{ij} e_{ij}(u_i) = 0 \tag{42}$$

and homogeneity of the loading functions enable calculating "reverse deformation" e_{ij} and the power of the external forces $\int_D \overline{s}_{ij}\, e_{ij}(u_i)dx = \int_D f_i u_i\, dx + \int_{\partial D_p} F_i u_i\, dS = \dot{}$. Once velocities u_i are defined, the displacements w_i are calculated per the formulas (25): this operation can be done within the space $B^{0*} = M$, if the ultimate states (36) are achieved the finite number of times during the deformation on the interval $0 \le t \le T$.

5. CONCLUSIONS

This paper demonstrates that the deformation process of the shape memory continuums is described within the theory of plasticity with two loading surfaces. Taking into account the link between the plastic flow and melting, shape restoration can be identified with melting at moderate temperature, whereas yield under high stress can be identified with melting under ultimate load. Different types of melting occur within one model, but each of them is satisfied with its own variational principle supported by external loads and deformation rates. The loads and temperatures are linked by the first and second laws of thermodynamics. The above conditions provide for existence of the generalized solutions and enable tracking the history of change in the continuum configuration. During the course of the evidence, it was proved that the deformed shape is not the only one. Additionally, the functions defining solutions to optimum problems, are often discontinuous.

The characteristics related to the ultimate analysis of the problems for the shape memory materials enable raising some questions that require further studies. First of all, it refers to the classification of the non-trivial solutions to the optimum problems (34)–(35) under additional restrictions on the continuum behavior, as well as identification of the conditions when discontinuous solutions occur. The direct methods of numerical analysis deserve further development because the finite-element method for the analysis of nonlinear extremum problems is often associated with loss of accuracy. The wide application of shape memory materials in many technical and scientific designs generates optimism for successful advancements in the above areas.

Acknowledgement/ Funding acknowledgement

The author(s) received no financial support for the research, authorship, and/or publication of this article.

Declaration of Competing Interest

The authors declare that they have no known competing financial interests or personal relationships that could have appeared to influence the work reported in this paper.

REFERENCES

[1] Otsuka, K., & Wayman, C. (1998). Shape memory materials. Cambridge University Press.

[2] Lagoudas, D. C. (Ed.). (2008). *Shape memory alloys: Modeling and engineering applications*. Springer Science & Business Media..

[3] Arun, D. I., Chakravarty, P., Arockia, K. R., & Snthosh, B. (2018). *Shape memory materials* (1st ed.). CRC Press.

[4] Panagiotopoulos, P. (1985). *Inequality problems in mechanics and applications*. Birkhäuser.

[5] Bonetti, E., Colli, P., Fabrizio, V., & Gilard, G. (2016). Existence of solutions for a mathematical model related to solid–solid phase transitions in shape memory alloys. *Archive for Rational Mechanics and Analysis, 219*(1), 203–254.

[6] Grachev, V. A., & Neustadt, Y. S. (2023). Mixed variational principle for shape memory solids. *Journal of Mechanics of Materials and Structures, 18*(5), 621–633.

[7] Abeyaratne, R., & Knowles, J. K. (2006). *Evolution of phase transitions: A continuum theory*. Cambridge University Press.

[8] Auricchio, A., Reali, U., & Stefanelli, U. (2007). A three-dimensional model describing stress-induced solid phase transformation with permanent inelasticity. *International Journal of Plasticity, 23*, 207–226.

[9] Frémond, M. (2012). *Phase change in mechanics*. Lecture Notes of the Unione Matematica Italiana, Springer.

[10] Cissé, C., Zaki, W., & Zineb, T. (2016). A review of constitutive models and modeling techniques for shape memory alloys. *International Journal of Plasticity, 76*, 244–284.

[11] Kachanov, L. M. (2004). *Foundations of the theory of plasticity*. Dover Publications.

[12] Mao-Hong, L., & Jian-Chun, L. (2012). *Structural plasticity*. Springer.

[13] Mosolov, P. P., & Miasnikov, V. P. (1981). *Mechanics of rigid plastic solids* (in Russian). Nauka.

[14] Kamenjarzh, J. A. (1996). *Limit analysis of solids and structures*. CRC Press.

[15] Nayroles, B. (1970). Essai de théorie fonctionnelle des structures rigides plastiques parfaites. *Journal de Mécanique, 9*(3), 491–506.

[16] Truesdell, C. A. (1972). *A first course in rational continuum mechanics*. Johns Hopkins University.

[17] Ziegler, H. (1981). Discussion on some objections to thermomechanical orthogonality. *Ingenieur-Archiv (Archive of Applied Mechanics, 50)*, 149–164.

[18] Born, M. (1939). Thermodynamics of crystals and melting. *Journal of Chemical Physics, 7*, 591–603.

[19] Furth, R. (1940). Relation between breaking and melting. *Nature, 3680*, 741–761.

[20] Luecke, W. E., Banovic, S. W., & McColskey, J. D. (2011). High-temperature

tensile constitutive data and models for structural steels in fire. *National Institute of Standards and Technology, Technical Note 1714*. Retrieved from http://www.nist.gov/manuscript-publication-search.cfm?pub_id=908536.

[21] Preisach, F. (1935). Über die magnetische Nachwirkung. *Zeitschrift für Physik, 94*(5-6), 277–302.

[22] Lagoudas, D. C., & Bhattacharya, A. (1997). On the correspondence between micromechanical models for isothermal pseudoelastic response of shape memory alloys and Preisach model for hysteresis. *Mathematics and Mechanics of Solids, 2*(4), 405–440.

[23] Ktena, A., Fotiadis, D. L., Spanos, P. D., & Massalas, C. V. (2001). A Preisach model identification procedure and simulation of hysteresis in ferromagnets and shape-memory alloys. *Physica B: Condensed Matter, 306*(1-4), 84–90.

[24] Yosida, K. (1965). *Functional analysis*. Springer.